ISSN 2745-3502
Volume 3 No. 1 – Oktober 2022
Indonesian Applied Physics Letters

# Ab Initio Molecular Dynamic Study of Structural and Electrical Properties of Gold Nanoparticle

Abdullah Aufa Fuad [1,a)], Andi Hamim Zaidan[1], Adri Supardi[1]

[1]Department of Physics, Faculty of Science and Technology, Universitas Airlangga Surabaya, East Java, Indonesia

[a)] a.aufa.f@gmail.com

**Abstract.** The goal of this research is to know structural and electrical properties of gold nanoparticle (GNP) through ab initio molecular dynamic (AIMD) method. Structural properties are explained by the study of coordination number, bond angle distribution, and radial distribution function. Electrical properties are explained by the study of band structure and density of states. GNP samples used in this research are liquid, amorph, and icosahedral. The main software used for AIMD numerical calculation was SIESTA. Liquid GNP is dominated by coordination number of 9, amorf GNP 10, icosahedral GNP 18. Bond angle distribution of liquid GNP has 1 peak in 60o, amorph GNP has 4 peak in 60o, 90o, 120o, 175o, icosahedral GNP has complete all 6 peak. Internal spacing of liquid GNP is 2,7 Å, amorph is 2,8 Å, icosahedral is 1,9 Å. Study of band structure show that the width of liquid GNP bandgap is 0,040 eV, amorph is 0,071 eV, icosahedral is 0,200 eV. While the width of bandgap by density of state study for liquid GNP is 0,053 eV, amorph is 0,085 eV, icosahedral is 0,200 eV.

## INTRODUCTION

In the past ten years, the growth of science has seen a surge in interest in nanotechnology. The field of nanotechnology is very vast and includes many different scientific fields. Nanotechnology can be employed in the medical field for fluorescent biolabeling, pathogen biodetection, protein and similar plasma detection in cells, DNA structure analysis, tissue engineering, tumor detection, cancer treatment, drug delivery, and gene delivery (Rajiv et al., 2012). Gold nanoparticles (GNP), one of the many forms of nanoparticles, are frequently used in studies. GNP, a precious metal, possesses qualities that make it biocompatible, including biological inertness, the ability to bioconjugate, regulated properties, and size in accordance with biological structures (viruses and bacteria) and molecules (proteins and DNA) (Chui, 2007).

It is well recognized that a nanoparticle's structure has a significant impact on how its properties, particularly GNPs, are regulated (Zhang et al., 2009). The structure of amorphous GNPs and their electrical characteristics will thus be investigated in this work. The distribution of tie angles, the depiction of structures, and radial distribution functions are a few structural topics that will be covered. Meanwhile, band structure and state density are studied in relation to electrical properties. It is highly challenging to conduct an experimental examination of the electrical characteristics and structure of nanoparticles. As a result, the widely adopted approach is the ab initio computation utilizing the density functional theory (DFT) simulation method.

## METHODOLOGY

This study will employ the SIESTA (Spanish Initiative for Electronic Simulations with Thousands of Atoms) software's ab initio computation technique. We'll give a brief overview of some of the key SIESTA features that are pertinent to this investigation. Software such as SIESTA, GNUPlot, AtomEye, and RINGS are required for this study.

## Treatment Concept

Three GNP samples—liquid, amorphous, and icosahedral—were employed in this work. The GNP is first heated at a temperature of 1500 K for 10 ps to create a liquid GNP sample. Given that the melting point of the Au atom is 1338 K at this moment, the GNP is entirely liquid. The liquid stage is the name given to this stage in this investigation.

The GNP was thereafter quickly cooled to 300 K. For 30 ps, the quenching process from 1500 K to 300 K was conducted. The quenching stage was then given to this phase. The GNP structure is now amorphous and relaxed at a steady temperature of 300 K for 10 ps when the temperature reaches this level. The amorphous stage is the name given to this phase. By entering the icosahedral coordinates and immediately relaxing it at a temperature of 300 K, the icosahedral GNP is created.

## *Pseudopotentials*

In SIESTA, the consequences of electron interactions with the nucleus are represented by pseudopotentials. The kind of functional exchange-correlation (XC) potential to be utilized determines the pseudopotential to be employed, and this functional type is reached by two sorts of techniques, namely GGA (Generalized Gradient Approximation) and LDA (Local Density Approximation). The pseudopotential used in this investigation was the pseudopotential LDA from Au since functional XC type LDA was employed (Artacho et al., 2012).

## Set Basis

The basis set is used by SIESTA to determine the Kohn-Sham equation's eigenvalues and eigenvectors. LCAOs are combined linearly to form this base set (localized numerical atomic orbitals). Simple, single (SZ), detailed, triple, and polarization (TZP) are just a few of the fundamental set possibilities that call for greater computer specs. A split type double and polarization (DZP) base set was utilized in this work (Artacho et al., 2012).

## Atom and Structure Input

Pada sampel likuid dan amorf disimulasikan sebanyak 80 atom Au. Sedangkan untuk sampel icosahedral disimulasikan sebanyak 147 atom Au. Ruang simulasi berupa kubus dengan konstanta kisi 12.177 Angstrom. Nilai konstanta kisi ditentukan dengan mempertimbangkan kerapatan sebenarnya dari 80 atom Au yakni 11.07 Angstrom ditambah 10%.

## Iteration Parameter

The iteration parameters used in this study are as in the Table 1.

**TABLE 1.** Iteration parameters of liquid and amorphous GNP

| Parameter | Value |
|---|---|
| MeshCutOff (likuid dan amorf) | 70 Ry |
| MeshCutOff (icosahedral) | 90 Ry |
| DM.Tolerance | 0.0001 |
| DM.NumberPulay | 3 |
| DM.MixingWeight | 0.1 |
| DM.UseSaveDM | .true. |
| Harris_functional | T |
| SolutionMethod | Diagonal |

## *Molecular Dynamic* (MD) Parameter

The MD parameters used in this study are as in Table 2 below.

**TABLE 2.** MD parameters of liquid GNP and amorphous GNP

| Parameter | Value | | |
|---|---|---|---|
| MD.TypeOfRun | Nose | | |
| MD.NoseMass | 200 | | |
| | liquid stage | Quenching stage | Amorf stage |
| MD.FinalTimeStep | 2500 | 7500 | 2500 |
| MD.LengthTimeStep | 4 | 4 | 4 |
| MD.InitialTemprature | 1500 K | 1500 K | 300 K |
| MD.FinalTemprature | 1500 K | 300 K | 300 K |

**TABLE 3.** Parameters of icosahedral GNP MD P

| Parameter | Value |
|---|---|
| MD.TypeOfRun | FIRE |
| MD.FIRETimeStep | 4 fs |
| MD.InitialTemprature | 300 K |
| MD.FinalTemprature | 300 K |
| MD.VariableCell | .true. |
| MD.RelaxCellOnly | .true. |

## Visualization

Each sample was seen using AtomEye successfully treated. The following images show how the visualization came out. The visible differences between the GNP structure in the liquid phase and the amorphous phase are minimal because of the exceptionally high density of gold.

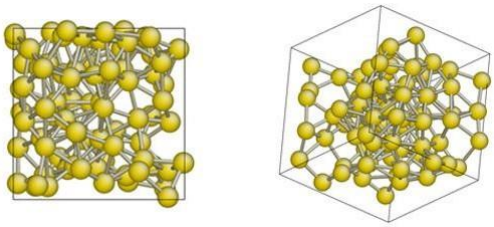

**FIGURE 1.** Visualization of liquid phase GNP structure, the same object is shown from 2 points of view

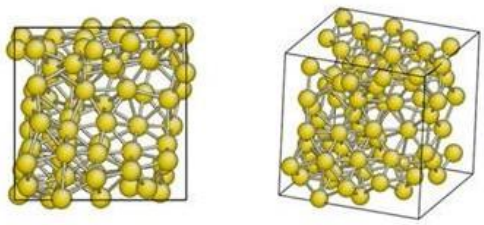

**FIGURE 2.** Visualization of amorphous GNP structure, the same object is shown from 2 points of view

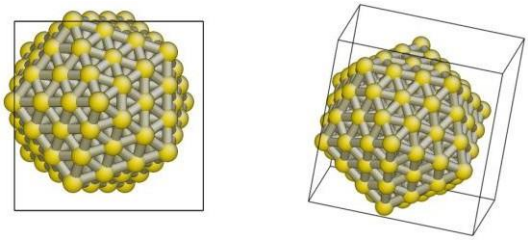

**FIGURE 3.** Visualization of the icosahedral GNP structure, the same object is shown from 2 points of view

There isn't a glaring difference between Figures 1 and 2, although Figure 1 appears slightly looser (no separate atoms from the main cluster). Distinction other variation that may be seen is in the number of atomic bonds, where in liquid GNP it is uncommon to find atoms with many bonds but common in amorphous GNP. Figure 3 below depicts the icosahedral GNP structure in graphic form.

## Bonding Total Numbers

The number of bonds of each atom is presented in the following figure with different color indicators based on the number.

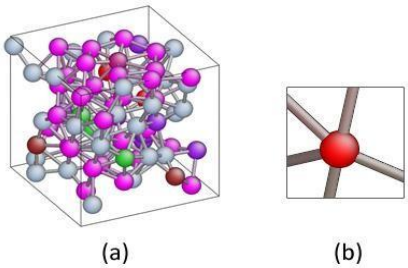


**FIGURE 4.** (a) visualization of the number of GNP bonds in the liquid phase, (b) examples of atoms that are has the number of bonds

From Figure 4, the following table 4 is obtained

**TABLE 4.** Total bonding numbers of GNP fase likuid

| Ikatan | Warna | Kuantitas | Persentasi |
|---|---|---|---|
| 5 | Merah | 2 | 2,5% |
| 6 | Coklat | 3 | 3,75% |
| 7 | Ungu | 8 | 10% |
| 8 | Biru muda | 30 | 37,5% |
| 9 | Merah muda | 33 | 41,25% |
| 10 | Hijau | 3 | 3,75% |
| 11 | Merah keunguan | 1 | 1,25% |

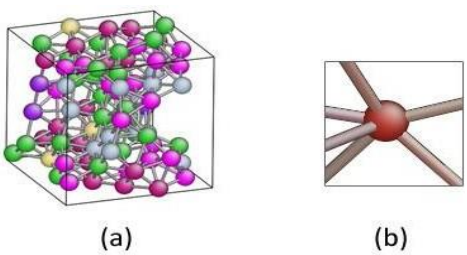


**FIGURE 5.** (a) visualization of the number of amorphous phase GNP bonds, (b) an example of an atom that has a 6 bond number

From Figure 5, the following table 5 is obtained as follows.

**TABLE 5.** Total bonding numbers of amorf

| Ikatan | Warna | Kuantitas | Persentasi |
|---|---|---|---|
| 7 | Ungu | 3 | 3,75% |
| 8 | Biru muda | 14 | 17,5% |
| 9 | Merah muda | 20 | 25% |
| 10 | Hijau | 25 | 31,25% |
| 11 | Merah keunguan | 15 | 18,75% |
| 12 | Kuning | 3 | 3,75% |

Figure 4.6 below illustrates the representation of the icosahedral GNP structure based on the number of bonds.

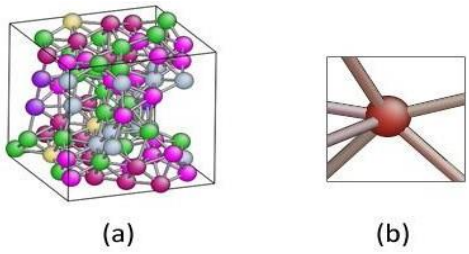


**FIGURE 6.** (a) visualization of the number of amorphous phase GNP bonds, (b) an example of an atom that has a 6 bond number

From Figure 6, the following table 6 is obtained as follows

**TABLE 6.** Number of icosahedral . GNP bonds

| Ikatan | Warna | Kuantitas | Persentasi |
|---|---|---|---|
| 6 | Coklat | 4 | 2,72% |
| 9 | Merah muda | 2 | 1,36% |
| 10 | Hijau muda | 30 | 20,41% |
| 12 | Merah keunguan | 23 | 15,65% |
| 13 | Biru | 20 | 13,61% |
| 14 | Merah tua | 4 | 2,72% |
| 15 | Biru laut | 4 | 2,72% |
| 16 | Abu-abu | 2 | 1,36% |
| 17 | Hijau tua | 26 | 17,69% |
| 18 | Kuning krem | 32 | 21,77% |

The number of bonds in icosahedral GNPs varies greatly, ranging from 6 to 18. This enormous number of variations is caused by the density of 147 gold atoms in the simulated box of 12.177 in addition to the fact that the icosahedral is an ordered standard structure. This information makes it possible to predict that icosahedal GNPs will have a lot of steep peaks in the tie angle distribution graph, which will be discussed later.

## Bond Angle Distribution

The magnitude of the bond angle offered with three atoms, which is then used as the x-axis, is plotted against the amount of the angle in percent, which is then used as the y-axis, to create the bond angle distribution graph.

The number of members in a certain group is growing, as is the group's overall size. The ring with only three persons is the simplest to complete because it is used so frequently in many different forms. This coin often

has a 60-degree knot angle, however there are also 90- and 45-degree versions. There are normally 3 types and 6 participants in the ring. The six member ring regular (type 1) has a hexagonal angle variation, but there is a situation in which three of the atoms in a type 3 ring cause the line to bend (angle 180o). Type 2 has a 120 degree angle on each side, whereas type 3 has a 150 degree angle on each side.

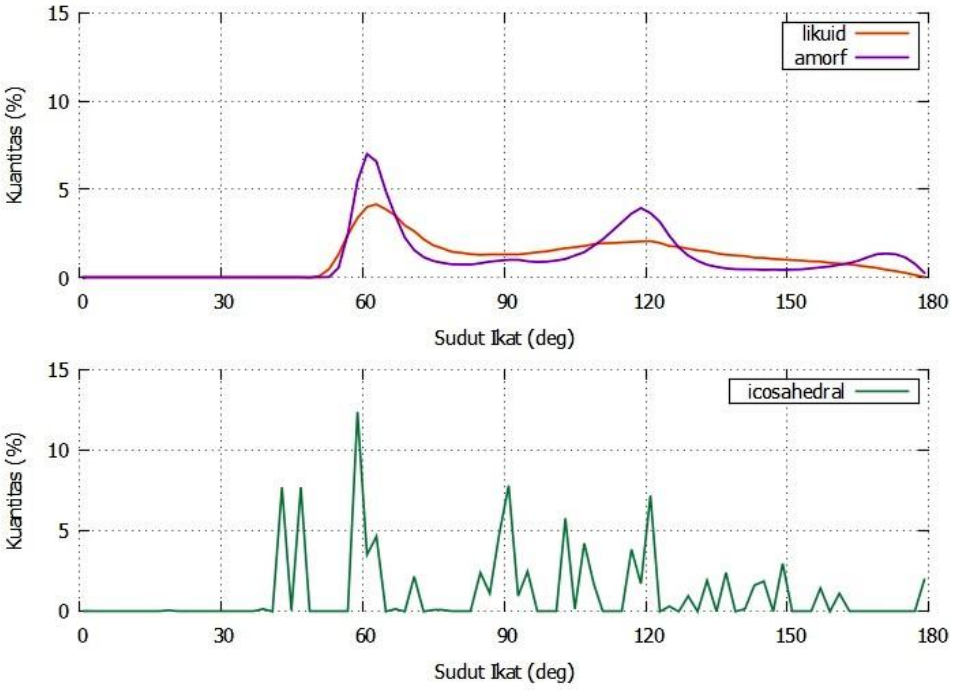


**FIGURE 7.** Graph of the distribution of the binding angles of the three samples.

Figure 7 depicts that, as compared to other phases, icosahedral GNPs have the sharpest peaks (high and narrow peaks) among the three tie angle distribution graphs. As a result, icosahedral GNPs are thought to have a wider range of structural fragments and typical binding angles than other GNPs. According to Chui (2007), a GNP peak will be less acute, wide, and low the more non-standard its structure is when it is generated [Chui, 2007].

There is only one peak in Graph 7 of the binding angle distribution of liquid phase GNPs, which is the peak in the 3-member ring (60o). This 60° angle is unusual but frequent in many different kinds of constructions. Therefore, the information at 60o cannot be used in isolation to anticipate the structure; the ownership of the peaks at other angles must also be defined. The peak in the ring of three members, four members (90o), six members of type one (120o), and six members of type three make up the amorphous GNP (175o-180o). Since there is no peak in the 4-member ring, there is no SC contribution or FCC (100) field in amorphous phase GNPs. The omission of a peak in the 6-membered type 2 ring underscores the SC structure's zero contribution and demonstrates that the amorphous GNP has no pentagonal contribution. According to the order of peak heights owned by amorphous GNPs, the dominant structure is a planar hexagonal, with peak heights starting at 60o, 120o, and 180o. Identical to this amorphous GNP with a ratio of 18:12:3, the hexagonal plane with the central atom in the centre will have three various bond angle variations.

The icosahedral GNP graph features a complete and distinct peak. The icosahedral GNP has six peaks in total, which are numbered from the peak in the 3-member ring to the peak in the 6-membered type 3 in that order. The occurrence of a full ring is the distinguishing feature that indicates that a graph of the distribution of the tie angle strongly implies the presence of an icosahedral structure. Visual observation reveals that the icosahedral GNP contains a large number of pentagonal sections that are rare in other samples. The icosahedral distribution graph, which contains the usual peaks of a 5-member ring at 100°, 110°, and 125°, supports this. Overall, the examination of the bond angle variations of the three samples supports the claim stated by Chui (2007) that the findings of bond angle analysis are dependent on the ordered-disordered crystal structure.

## Radial Distribution Function

FDR analysis is required to learn about the interior structure of these Au atoms because they form a tight configuration. The FDR graph is a graph with the radial distribution function where r is the number of angstroms as the y-axis and the distance (r) as far as the number of angstroms from the central atom as the x-axis.

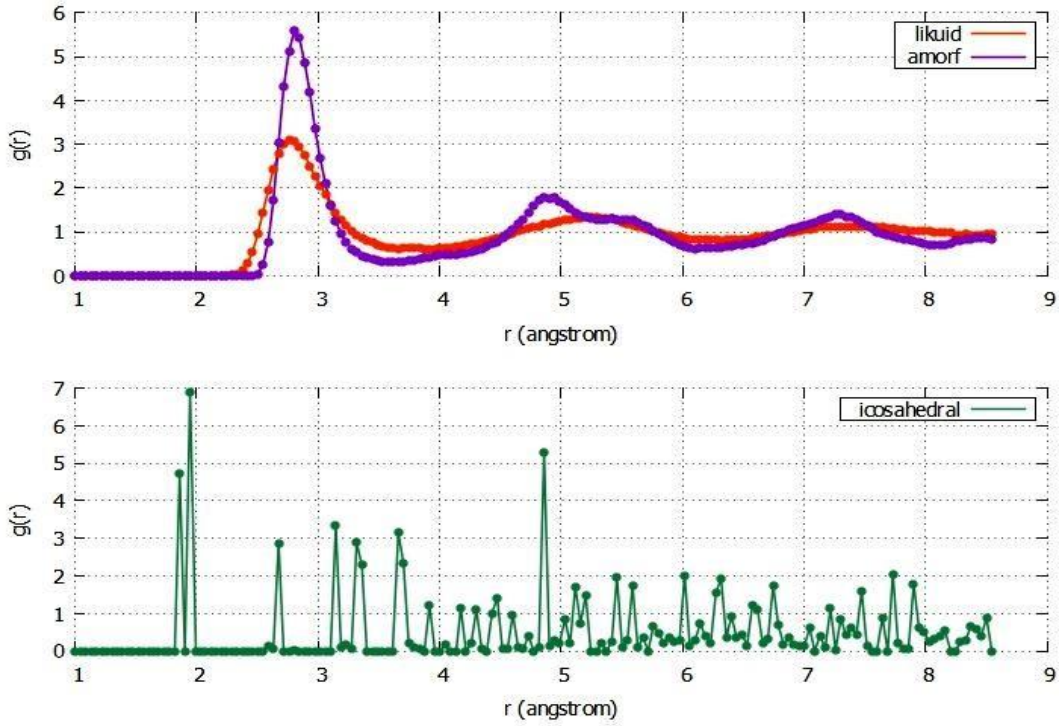


**FIGURE 8.** FDR graph of the three samples

The internal gap of the liquid phase FDR graph, which is represented by the first peak in Figure 4.9, is 2.7, while the internal gap of amorphous GNP is 2.8. This means that the closest atom is discovered after a gap or distance of 2.8, as is the case with 2.7 in liquid phase GNP, for instance, if there is a central atom in the centre of the coordinates of amorphous GNP. The increased packing freedom in the liquid phase is the reason the internal gap of the GNP is narrower than that of the amorphous GNP. To optimize its cohesive energy, the atom could interact with any other atom as closely as possible owing to the enhanced packing freedom [Chui, 2007].

There is a striking difference at the top of the two liquid graphs and amorphous graphs. In the amorphous graph, both peaks are wide and branched, meaning that there is a contribution of glassy structures to amorphous GNPs which of course will not be found during liquid phase GNPs, because the second peak of FDR when wide and branched is a typical characteristic of glassy structures [Qi, 1999].

At 1.9, icosahedral GNP reaches its initial peak. The icosahedral GNP has the smallest internal gap (1.9), but this value cannot be assigned to the liquid or amorphous GNPs since the icosahedral GNP has an ordered crystalline structure, whereas the liquid and amorphous GNPs do not. In addition, the icosahedral GNPs' crystal structure is significantly compacted, resulting in a small internal gap, due to the higher number of atoms (147) in the same volume simulation box as the amorphous and liquid GNPs (80). There are two different atomic densities that are relatively close to the core atom when the branching finishes at the first peak of an icosahedral GNP. These two densities indicate two various sorts of rings separated by only 0.1. The explanation of the six icosahedral symmetries in Figure 4.3, which may be broadly divided into two types of nearest neighbor arrangements, strengthens the claim that there are two rings. This can be explained by the fact that the FDR is equal to 4.8 at a distance of 1.8 from the central atom, which indicates that the atomic density is 4.8 times higher than the average density. The location of the first ring is here. The FDR is 7.9 only 0.1 seconds later. The second ring is located here. The first branching peak phenomena in this simulation shows that the icosahedral structure was over compressed.

## Density of State

The SIESTA output's eigenvalue data, which can be found in a file with the extension, is used to create the state density graph 9. The file is then transformed into state density data that is prepared for graphing. The x-axis of the density of states graph represents the energy (eV) of the energy state that an electron will inhabit, and the y-axis is the number of energy levels that an electron may occupy. The following table displays the raw data output of the eigen values before processing.

**TABLE 7.** Output eigenvalues that will be plotted on the state density graph

| Sampel | Npita | E min | E max | E Fermi |
|---|---|---|---|---|
| Likuid | 1200 | -53,17 | 48,65 | -0,22 |
| Amorf | 1200 | -40,67 | 48,74 | -0,98 |
| Icosahedral | 2205 | -30,78 | 146,01 | 7,52 |

Only those in the Fermi energy range can have their band gap value calculated out of the tens of thousands of energy bands that are examined. The number of energy bands that can be plotted on the graph is 1000. The entire value of the Fermi energy is then shifted to the value x=0 for the sake of graphic order. The plot is made in the region of -1 eV to 1 eV with 0.01 eV precision after the Fermi energy is adjusted to zero. The plot's outcomes are depicted in Figure 4.9 down below.

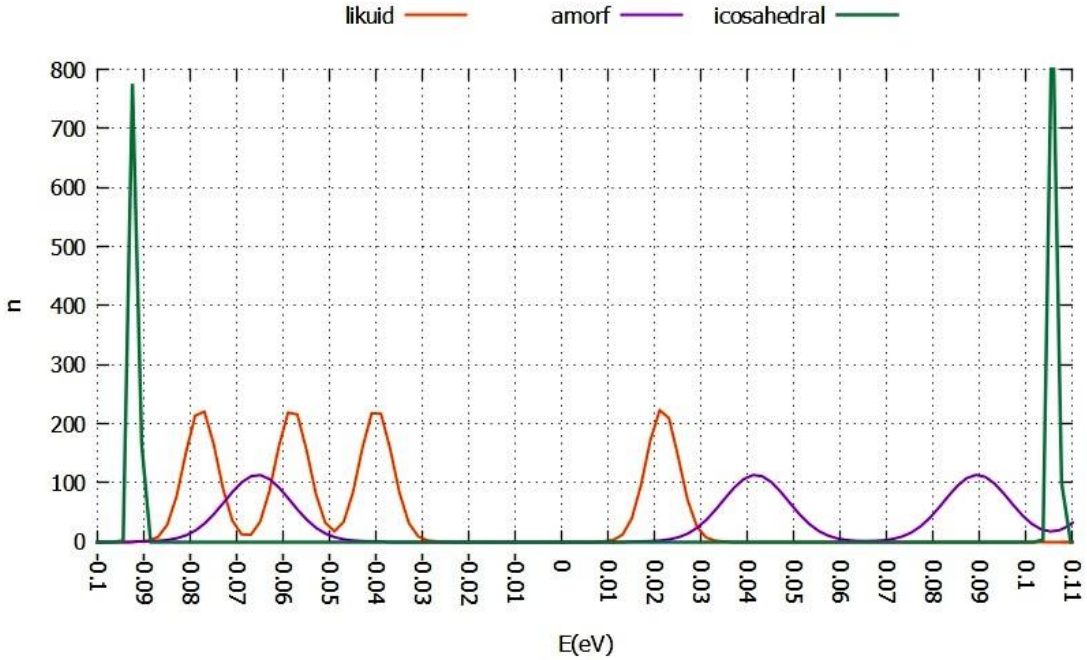


**FIGURE 9.** Graph of the density of the GNP conditions of the three samples.

The energy band gap width for GNP in the liquid phase is 0.040 eV (0.010+0.030), as can be observed from the graph. Amorphous GNP has a band gap width of 0.071 eV (0.023+0.048). Given the narrow slit, GNP must be a good conductor. The gap width of the icosahedral GNP is 0.200 eV (0.112+0.088), which is wider than that of the other samples. Icosahedral, amorphous, and liquid GNPs are listed in order of decreasing gap width. The density of the locations between the atoms affects the gap's breadth. The difficulty of electrons travelling and flowing will be affected if an atom is too close to its nearest neighbor atom (nearest neighbor) (current). The adjacent property. The FDR sub-chapter has examined the closest neighbor. The icosahedral GNP has the lowest internal gap among the other samples, according to the FDR study's findings, meaning that it has the closest neighbor position.

## Band Structure

The relationship between wavenumber k on the x-axis and the quantity of energy on the y-axis is shown in Figure 10 to illustrate the band structure. Figure 10 below provides a detailed graph of the energy band structure in the Fermi energy range (not shifted to zero). The conduction band is located above the Fermi energy and the valence band is located below it. The band gap value is indicated by the space between the two bands.

The energy band gap width for GNP in the liquid phase is 0.053 eV, as can be shown in Figure 10 below (0.262-0.209). Amorphous GNP has a band gap width of 0.085 eV. (0.996-0.911). Given the narrow slit, GNP must be a good conductor. The icosahedral GNP, on the other hand, has a 0.200 eV greater slit width than the other samples (7.621-3.421).

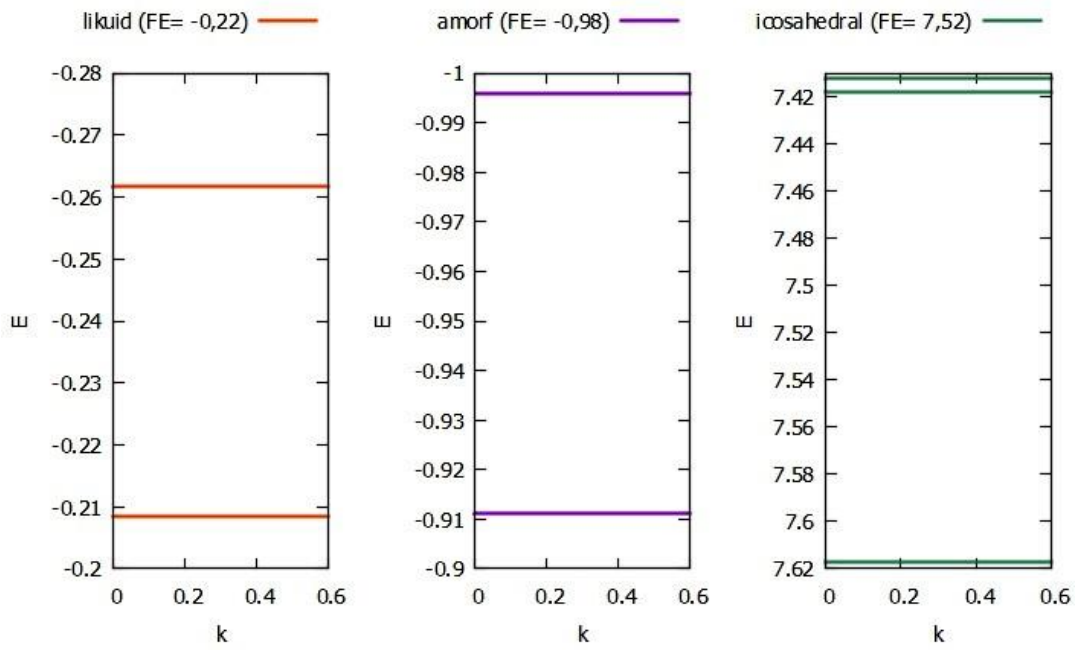


**FIGURE 10.** GNP energy band gap of the three samples.

Similar to the previous assessment, it is also evident that icosahedral, liquid, and amorphous GNPs have the smallest to biggest band gaps. The mean free path, or MFP, as well as the reason for the nearest neighbor atom, help to explain this. According to Marion (2011), MFP is the average distance that particles (such as atoms, photons, and electrons) travel between collision distances with other particles that can result in changes to direction, energy, or other attributes. The MFP will actually narrow as a result of an overly tight crystal structure, which will have ramifications for the electrons' increasingly non-free route. The electrons are more challenging to flow the less free the direction they travel. Or to put it another way, the conductivity drops.

The correlation of the spectrum gap value in between results from the reviews of the bandgap and density for the three samples reveals a very excellent convergence with just a variation of 0.013 to 0.014 eV. The comparison is tabulated in figure 4.5 below.

**TABLE 8.** Bandgap values for comparison of the two reviews

| Sampel | Celah Pita | |
|---|---|---|
| | Struktur Pita | Rapat Keadaan |
| Likuid | 0,053 eV | 0,040 eV |
| Amorf | 0,085 eV | 0,071 eV |
| Icosahedral | 0,200 eV | 0,200 eV |

## CONCLUSION

Since the outcomes will convergence with the dispersion of the bond angles, the more bonds there are, the more variability there will be in the binding angle. The degree of order and irregularity in the crystal structure affects how the bond angles are distributed. Due of the high degree of packing freedom, the atoms are forced to form the tightest feasible bonds in order to maximize cohesive energy, which also dictates the internal gap. The mean free path, which impacts the conductivity, and the internal gap are both directly proportional. According to the density study, the band gaps of liquid, amorphous, and icosahedral GNPs were, respectively, 0.040 eV, 0.071 eV, and 0.200 eV. Band gap measurements of liquid, amorphous, and icosahedral GNPs revealed by band structure analysis were 0.053 eV, 0.085 eV, and 0.200 eV, respectively. This information reinforces the previous point.

## REFERENCES

1. Artacho, Emilio, dkk. 2013. User's Guide SIESTA 3.2. Universidad Aut´onoma de Madrid.
2. Artacho, Emilio, dkk. 2002. The Siesta method for ab initio order-N materials simulation. J. Phys. Cond. Matt. 14, 2745.
3. Jorge Botana Alcalde. 2011. Ab initio study of low-dimensional metallic systems. PhD Thesis. Universidade de Santiago de Compostela.
4. Juh Tzeng Lue. 2007. Physical Properties of Nanomaterials. Encyclopedia of Nanoscience and Nanotechnology. Volume X. 1-46.
5. W.Kohn, L.J Sham. 1995. Self-Consistent Equation Including Exchange and Correlation Effect. J. Phys.Rev. 140
6. Yu Hang Chui. 2007. Molecular Dynamics Study of Structure and Stability in Au Nanoparticles. PhD Thesis. RMIT University. Melbourne, Australia.
7. Jin Zhong Zhang. 2009. Optical Properties and Spectrosopy of Nanomaterials. University of California. Santa Cruz; USA.